



## Non-destructive evaluation methods for degradation of IG-110 and IG-430 graphite

Taiju Shibata<sup>a,\*</sup>, Junya Sumita<sup>a</sup>, Tatsuya Tada<sup>b</sup>, Satoshi Hanawa<sup>b</sup>, Kazuhiro Sawa<sup>a</sup>, Tatsuo Iyoku<sup>a</sup>

<sup>a</sup> High Temperature Fuel and Material Group, Japan Atomic Energy Agency, 4002 Oarai-machi, Ibaraki-ken 311-1393, Japan

<sup>b</sup> Technology Development Division, Japan Atomic Energy Agency, 4002 Oarai-machi, Ibaraki-ken 311-1393, Japan

### A B S T R A C T

The lifetime extension of in-core graphite components is one of the key technologies for the VHTR. The residual stress in the graphite components caused by neutron irradiation at high temperatures affects their lifetime. Although oxidation damage in the components would not be significant in normal reactor operation, it should be checked as well. To evaluate the degradation of the graphite components directly by a non-destructive analysis, the applicability of the micro-indentation and ultrasonic wave methods were investigated. The fine-grained isotropic graphites of IG-110 and IG-430, the candidate grades for the VHTR, were used in this study. The following results were obtained. (1) The micro-indentation behavior was changed by applying the compressive strain on the graphite. It suggested that the residual stress would be measured directly. (2) The change of ultrasonic wave velocity with 1 MHz by the uniform oxidation could be evaluated by the wave-propagation analysis with wave-pore interaction model. (3) The trend of oxidation-induced strength degradation on IG-110 was expressed by using the proposed uniform oxidation model. The importance of the non-uniformity consideration was indicated.

© 2008 Elsevier B.V. All rights reserved.

### 1. Introduction

The very high temperature reactor (VHTR) is a promising candidate for the Generation IV nuclear energy system [1]. It can provide high temperature coolant helium gas above 950 °C at the reactor outlet. It can be used at nuclear heat utilization systems, hydrogen production, and power generation by gas turbine systems, for example. Graphite materials are used for core components of the VHTR because of their superior heat resistance. Residual stress is caused in the graphite components by neutron irradiation at high temperatures through the reactor operation, and it affects their lifetime. The components are also gradually oxidized in the reactor by quite a small amount of impurity gases in the coolant helium even during normal operation. The evaluation of this damage on the graphite components is one of the key technologies for their lifetime extension [2–4].

The Japanese VHTR system GTHTR-300C [5] adopts a block type core design similar to the high temperature engineering test reactor (HTTR), which is the first HTGR in Japan with the maximum thermal power of 30 MW [6]. The fine-grained isotropic IG-110 graphite (Toyo Tanso Co.) is used in the HTTR core, and the IG-110 (IG-11) and IG-430 (Toyo Tanso Co.) are candidates for the VHTR graphite components. Since the fuel elements and graphite components of the VHTR will be used at more stringent conditions

than that of the HTTR, it is important to confirm their structural integrity to extend their lifetime.

The residual stress of the components is generally analyzed by the irradiated neutron fluence and material database from the previous irradiation experiments. The lifetime of the components is determined by comparing the analytical results, which contains safety margin, with the allowable stress limit of the graphite. If we can measure the residual stress directly by a non-destructive method, the margin would be reduced reasonably, and hence the argument for extending the working lifetime of the components would be strengthened. For this purpose, we are developing a measuring method for the residual stress on graphite blocks directly by using a micro-indentation technique. Since the indentation behavior is affected by the residual stress condition, it would be possible to evaluate the stress condition by the micro-indentation test. Ishihara and Oku [7] showed the possibility of the micro-indentation method to the tensile stress condition of the IG-110 graphite. It is necessary to check the applicability of the micro-indentation technique to the compressive condition as well.

Although the oxidation damage in the components would not be significant in normal reactor operation, it should be checked to extend their lifetime. The oxidation changes the inner porous condition of the graphite components that leads to their degradation. Since the ultrasonic testing is applicable to porous ceramics including graphite materials, it would be used to evaluate the inner porous condition. The wave propagation characteristics in the graphite components are affected by the inner porous conditions, such as porosity and pore size, which is changed by the oxidation.

\* Corresponding author. Tel.: +81 29 266 7705; fax: +81 29 266 7710.  
E-mail address: [shibata.taiju@jaea.go.jp](mailto:shibata.taiju@jaea.go.jp) (T. Shibata).

Therefore, it would be possible to evaluate oxidation damage by wave propagation characteristics. Shibata and Ishihara [8] showed the possibility of the wave propagation analysis to the oxidation damage evaluation by using the existing data with frequency of 2.25 MHz [9]. However, it is important to use the lower frequency to reduce the attenuation loss in the graphite block.

In this paper, the developing micro-indentation method to evaluate the residual compressive stress is described. The applicability of the ultrasonic wave method on oxidation damage evaluation is discussed with newly obtained experimental data with frequency of 1 MHz.

## 2. Experimental

### 2.1. Graphite specimens

The two grades of fine-grained isotropic graphites, IG-110 made from petroleum coke and IG-430 made from coal tar pitch coke, are focused on in this study. They are isotropic graphites manufactured by the isostatic pressing method (Toyo Tanso Co.) and candidates for the in-core graphite components of the VHTR. Typical material properties of IG-110 and IG-430 graphites are shown in Table 1. Two types of specimens were prepared. One is a large block type specimen with  $100 \times 200 \times 290$  mm sides to measure the specific ultrasonic wave velocity for both the graphites. The other is a relatively small type specimen with  $10 \times 10 \times 10$  mm sides to measure the micro-indentation behavior and oxidation effects on wave propagation characteristics for the IG-110.

The surface oxidation of graphite occurs above about  $800^\circ\text{C}$  and the inner oxidation occurs below that temperature. For the oxidation test, the small type specimens were heated in a furnace with inducing air at  $500^\circ\text{C}$  to attain the uniform inner oxidation. The oxidation ratio, burn-off, was changed as a parameter from 0% to 10%. The burn-off  $B$  is determined by specimen weight  $W_0$  and  $W$ , respectively before and after the oxidation as

$$B = (W - W_0) / W_0. \quad (1)$$

The surface condition was observed by a scanning electron microscope (SEM).

### 2.2. Micro-indentation test

The micro-indentation behavior at the compressive strain condition was measured. The test apparatus is shown in Fig. 1. The residual compressive strain on the IG-110 graphite with  $10 \times 10 \times 10$  mm sides was simulated by applying compressive load on the specimen in the horizontal direction. The compressive strain was measured by the strain gage attached on the side surface of the specimen. A diamond spherical shape indenter with 0.5 mm in radius and a Vickers indenter were used. The maximum indentation load was 2 N. The relationship between indentation

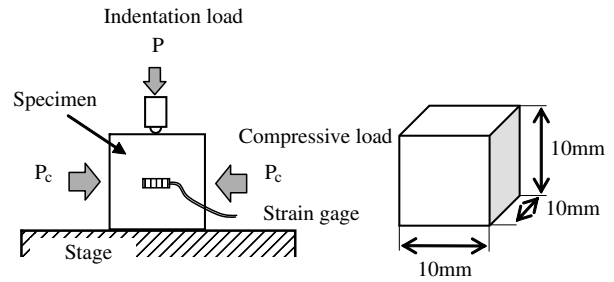


Fig. 1. Test apparatus for micro-indentation test at compressive condition.

load and indentation depth was continuously recorded by a DUH-201 (SHIMADZU Co.) unit.

### 2.3. Ultrasonic wave measurement

The ultrasonic wave propagation characteristics were measured by a digital ultrasonic testing machine (USI-550, Krautkramer) and the waveforms were recorded in it. The reflection method with 1 MHz of longitudinal wave was used for the measurement. Probes were 6 mm in diameter for the small specimens ( $10 \times 10 \times 10$  mm) and 24 mm in diameter for the large block type specimens ( $100 \times 200 \times 290$  mm).

## 3. Analysis

A wave-pore interaction propagation model [10] for the propagation analysis shown in Fig. 2 is used for the graphite specimen. Spherical pores with a radius  $r_0$  are assumed to be located uniformly in the specimen. When a wave comes into collision with a pore, it will go forward creeping through the pore surface, as a creeping wave, with a probability determined by porous conditions. The creeping process causes a time delay compared to the direct wave. The wave propagation characteristics are analyzed by cumulating the time delay and the collision probability with a great number of pores. The sound velocity  $V_0$  of the porous body is evaluated as a normalized value by that of the ideal polycrystals without pore  $V_i$  as follows [10]:

$$V_0/V_i = 1/\{1 + 3\phi_0(\pi\beta_0/\alpha_0 - 2)/8\}, \quad (2)$$

$$\alpha_0 = V_c/V_p, \quad (3)$$

$$\beta_0 = 4L_p/(2\pi r_0), \quad (4)$$

where  $V_c$  and  $V_p$  are respectively velocities of the creeping and direct waves,  $4L_p$  a perimeter of the pore and  $\phi_0$  a porosity. The velocity after the oxidation  $V$  is expressed as follows:

$$V/V_0 = \frac{1 + 3\phi_0(\pi\beta/\alpha - 2)/8}{1 + 3\phi(\pi\beta/\alpha - 2)/8} \quad (5)$$

where  $\beta/\alpha$  expresses the value after the oxidation.

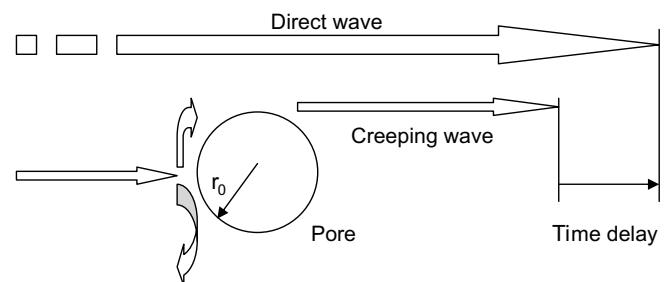


Fig. 2. Wave-pore interaction model for propagation analysis [10].

Table 1  
Typical material properties of IG-110 and IG-430 graphites

Material	IG-110	IG-430
Bulk density ( $\text{Mg}/\text{m}^3$ )	1.78	1.82
Tensile strength (MPa)	25.3	37.2
Compressive strength (MPa)	76.8	90.2
Young's modulus (GPa)	8.3	10.8
Poisson's ratio	0.14	-
$S_u$ value for tensile (MPa)	19.4	-
$S_u$ value for compressive (MPa)	61.4	-

$S_u$ : Specified minimum ultimate strength is determined from statistical treatment of strength data such that the survival probability is 99% at a confidence level of 95%.

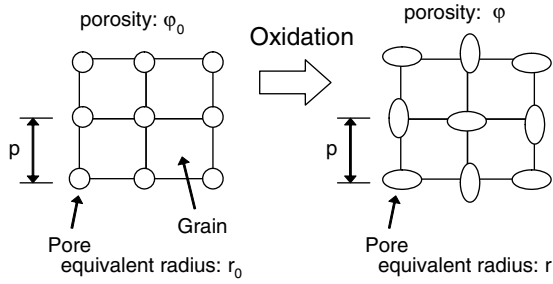


Fig. 3. Pore growth model for uniform oxidation.

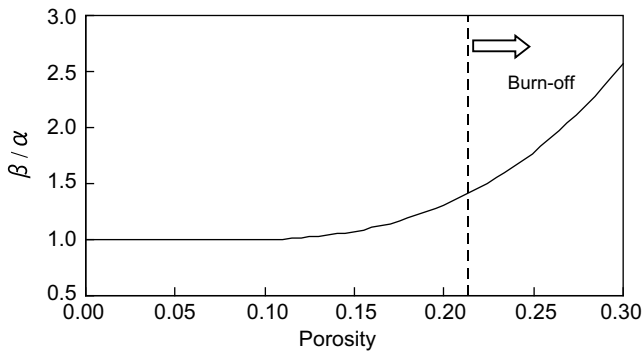


Fig. 4.  $\beta/\alpha$  Value for IG-110 graphite as a function of porosity.

To evaluate the wave propagation characteristics for oxidized graphite, we propose the pore growth model by uniform oxidation as shown in Fig. 3. At the un-oxidized condition with porosity of  $\phi_0$  as shown in the left figure, the spherical pores having unique pore radius  $r_0$  are assumed to be distributed uniformly with pitch  $p$ . The grain size is assumed as unique. After the uniform oxidation in the right figure, it is assumed that the pores become large at the same position and their shape changes to the non-spherical one. The pore oxidation ratio is assumed as unique for every pore and the pore size is expressed by the equivalent radius  $r$ .

The pore shape change by oxidation affects the  $\beta/\alpha$  value in Eq. (5). Shibata and Ishihara [8] showed that the change of the  $\beta/\alpha$  value for IG-110 graphite by uniform oxidation can be expressed as a function of porosity by modifying the empirical relationship for the alumina samples [10]. Fig. 4 shows the  $\beta/\alpha$  value for IG-110 graphite as a function of porosity. For the IG-110 graphite, its porosity at un-oxidized condition is about 0.21. When the pore shape is changed to the non-spherical shape after oxidation, the  $\beta/\alpha$  value increases with increasing the porosity. The region above the porosity of 0.21 shows the oxidized condition.

## 4. Results and discussion

### 4.1. Micro-indentation behavior

Fig. 5 shows the typical experimental result of the indentation load–depth relationship on IG-110 by the micro-indentation test. Compressive strain on the specimen was given by applying the compressive load. The compressive strain of 0.2% in the figure corresponds to about 12 MPa of compressive stress which is about 20% of the specified minimum ultimate strength 61 MPa of IG-110. At the level of the indentation load of 2 N, we can see that the maximum depth decreases with increasing compressive strain. It can be said that the resistance of the graphite specimen against the indentation load is increased by applying the compressive

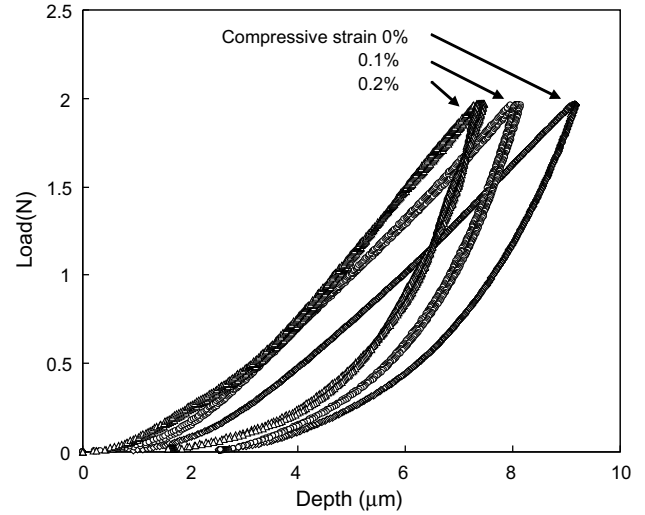


Fig. 5. Micro-indentation test result of indentation load–depth relationship on the IG-110 at compressive condition.

strain. It indicates that the compressive stress condition would be evaluated by the load–depth behaviour of the micro-indentation test.

The present authors have analyzed the maximum indentation depth with the spherical indenter in relation to the compressive strain on IG-110 by using the ABAQUS code [4]. It was analytically shown that the change of the indentation depth is expressed by using the compressive strain  $\varepsilon$  as

$$\delta = -1.11 \times 10^7 \varepsilon^3 + 7.20 \times 10^4 \varepsilon^2 - 1.66 \times 10^2 \varepsilon + 1 \quad (0 \leq \varepsilon \leq 0.0035), \quad (6)$$

where  $\delta$  is the normalized indentation depth of that for the un-stressed condition. The indentation depth decreases with increasing compressive strain, and the  $\delta$  is evaluated as about 0.85 at the compressive strain of 0.3%, for instance. Although the experimental data for the indentation depth, which was obtained by the above method, contain relatively large scattering, the analysis can trace the trend of the decrease in relation to the compressive strain [4]. As for the scattering, it is probably caused by the relatively small indentation load 2 N. In this case, the indentation depth is less than 10  $\mu\text{m}$ , as shown in Fig. 5. It is almost a half of the average grain size of IG-110, and the indentation behaviour must be affected by the surface roughness condition. Since the indentation behaviour is generally affected by the region which is several times larger than the indented area, it is expected that the scattering would be reduced by using the larger indentation load. It will be carried out in the next step of the study.

### 4.2. Burn-off conditions

Fig. 6 shows the differences in surface conditions of IG-110 specimens as a function of burn-off. The burn-off of each specimen was changed as a parameter. For the un-oxidized specimen, burn-off 0%, small pores can be observed. The porosity of IG-110 graphite is about 0.21 at this condition. It is obvious that the surface condition becomes rougher with increasing burn-off. In the figure of burn-off 1% e.g., we can easily see the oxidation damage proceeded uniformly.

Sato et al. [9] reported that the temperature difference of 5 °C at burn-off temperature 600 °C gives the difference of burn-off speed of 15% and they obtained relatively uniform burn-off specimens of IG-110 at 600 °C with careful treatment. Since our burn-off test

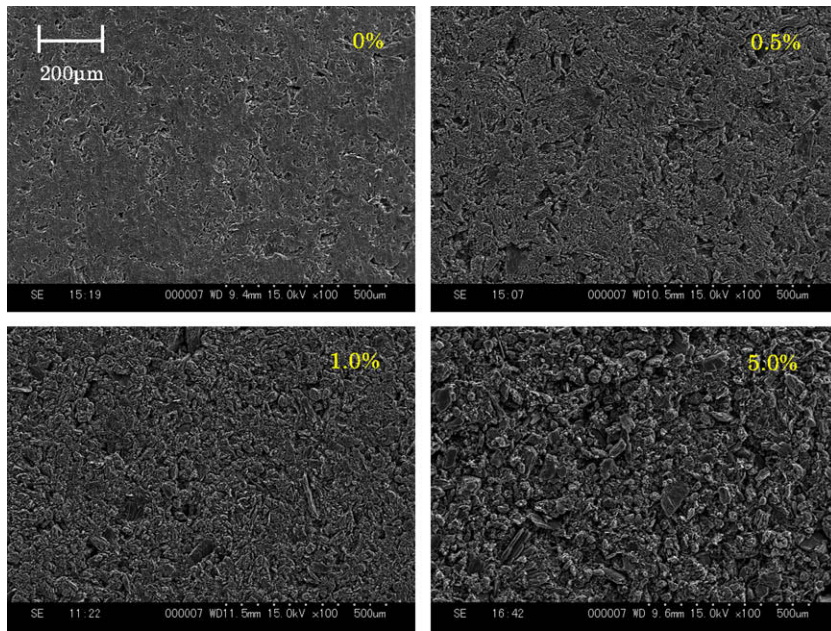


Fig. 6. Difference of surface condition of IG-110 specimens by burn-off (0, 0.5, 1.0 and 5.0%).

was carried out at 500 °C, the burn-off in this experiment must give uniform oxidation. We obtained the uniform oxidized IG-110 specimens for the ultrasonic wave propagation test.

#### 4.3. Oxidation damage evaluation by wave propagation characteristics

The sound velocities of IG-110 and IG-430 graphites with the large block type specimen with  $100 \times 200 \times 290$  mm sides were measured. For the propagation length of 290 mm, the average velocity of the 14 blocks is 2380 and 2520 m/s for IG-110 and IG-430, respectively. They respectively have the standard deviation of 35 and 20 m/s. The velocity of the IG-430 is about 6% greater than that of the IG-110. It is probably a result of the difference in the raw materials and the bulk densities, as shown in Table 1.

The porosity of IG-110 graphite is about 0.21 and it increases by oxidation. The increase of the porosity affects the wave propagation characteristics. The oxidation effect on velocity was analyzed by Eq. (5) and the change of wave velocity by the burn-off is shown in Fig. 7. The experimental data is also plotted in the figure. The velocity is expressed as the normalized value of the velocity with un-oxidized condition. The analysis shows that the velocity decreases with increasing burn-off. By comparing the analytical results and the experimental data, although there is some

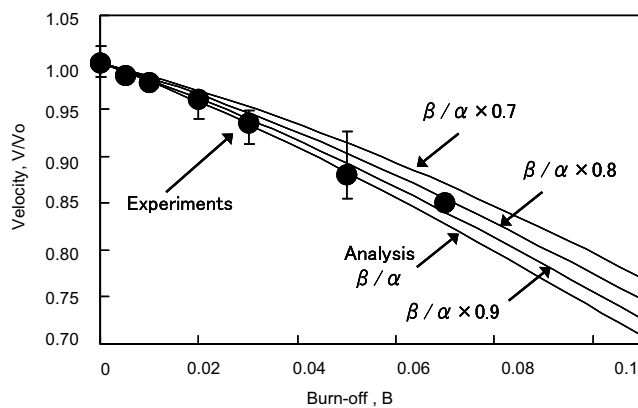


Fig. 7. Change of wave velocity by the burn-off ( $10 \times 10 \times 10$  mm small sample).

scattering of the data at the burn-off above 5%, the analysis with original  $\beta/\alpha$  is seemed to be in good agreement with the experimental data. It should be noted here that the data was obtained by the  $10 \times 10 \times 10$  mm small sample. The measurement error for the velocity and oxidation weight loss would not be small in Fig. 7. The sample size dependency should be evaluated by using large blocks in the next study.

The effect of the different pore shape coefficient by the burn-off was also evaluated in the analysis. The analytical result are also shown in Fig. 7 by multiplying factors parametrically on the original  $\beta/\alpha$ . We can see that the smaller factor,  $V/V_0$ , is derived from the pores of which deviation from spherical shape is small. For the spherical pores, the decrease of the velocity is lower than for the non-spherical pores, the decrease of the velocity is lower than for the non-spherical pores. At the relatively low burn-off region below 3%, the analytical result with original  $\beta/\alpha$  is seemed to be in good agreement with the experimental results for the small sample. It is indicated that the oxidation damage could be evaluated by the wave-propagation analysis when the uniform oxidation assumption is applicable. This point will be investigated with large blocks in the next study.

Fig. 8 shows the change of surface structures of IG-430 by the oxidation up to the burn-off of 2%. The SEM images were observed at the same area by checking the mark shown in the upper right corner. It can be said that the oxidation was progressed uniformly at the surface. For the IG-430 graphite, the progress of the oxidation damage is almost the same as the IG-110. It suggested that the wave propagation analysis model for the graphite is basically applicable to the IG-430 as well.

#### 4.4. Strength evaluation with proposed oxidation model

At the uniform oxidation condition, the degradation of the mechanical properties of graphite can be evaluated by the burn-off. Sato et al. [9] investigated the variation of the mechanical properties of graphite materials due to the uniform oxidation and proposed empirical formulas to express the variation. The variation of the mode-I fracture toughness for IG-110 graphite with the uniform oxidation is empirically expressed by the burn-off  $B$  as follows:

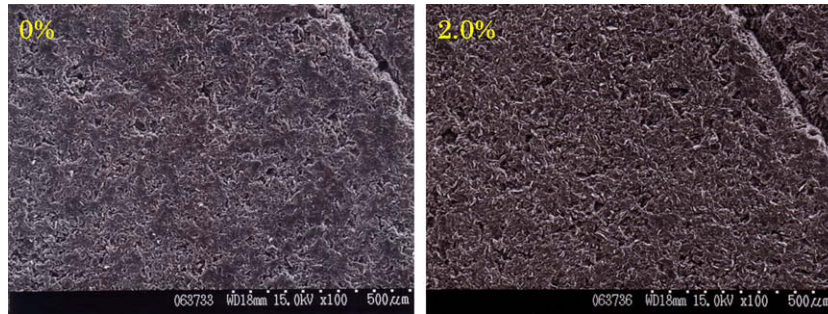


Fig. 8. Change of surface structures of IG-430 by burn-off (0 and 2.0%).

$$K_{IC} = 0.723 \exp(-5.27B), \quad (7)$$

where  $K_{IC}$  is the mode-I fracture toughness value.

Shibata and Ishihara [11] proposed the pore-related crack concept to evaluate the oxidation-induced degradation of the strength of the graphite. Since pores can be regarded as the initiation and/or extension sites of cracks in the graphite, the crack size is expected to depend on the pore size. The tensile strength is hence expected to decrease with increasing pore size. The tensile strength can be evaluated as a function of crack size by the following well-known equation in fracture mechanics:

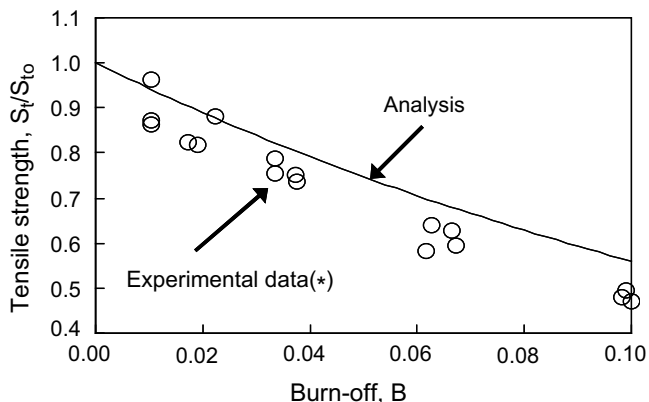
$$S_t = K_{IC} / \sqrt{\pi C_e}, \quad (8)$$

where  $S_t$ ,  $K_{IC}$  and  $C_e$  are the tensile strength, the mode-I fracture toughness and the effective crack size, respectively. In our uniform oxidation model, proposed in Fig. 3, it is considered that the effective crack length is proportional to the effective pore size. In this case, the degradation of tensile strength of IG-110 can be expressed as follows:

$$S_t/S_{t0} = K_{IC}/K_{IC0} \cdot \sqrt{r_0/r} = \sqrt{r_0/r} \cdot \exp(-5.27B). \quad (9)$$

The subscript 0 means the value for the un-oxidized condition.

Fig. 9 shows the change of tensile strength of IG-110 as a function of burn-off. The analysis was carried out by Eq. (9). The experimental data in the graphite structural design code for the HTTR [12] was also plotted in the figure. The strength decreases with increasing burn-off, i.e. with increasing pore size. Although the analytical results show slightly higher values than those of the experiments, the analysis is in agreement with the experimental data. It is suggested that our proposed oxidation model is basically applicable to evaluate the uniform oxidation damage. It is probable that the oxidation damage was not fully uniform in the experi-



(\*) Ishihara, et al., JAERI-M 91-153 (1991).

Fig. 9. Change of tensile strength of IG-110 as a function of burn-off.

ment, and hence it gave larger pores than those proposed in the uniform pore model. It would result in more severe degradation in the experiment than in the analysis. It is necessary to consider non-uniform oxidation damage on mechanical property degradation in the next step.

## 5. Conclusions

Lifetime extension is one of the key issues of graphite components in the VHTR. To evaluate the degradation of the graphite directly by a non-destructive method, the applicability of micro-indentation and ultrasonic wave methods was investigated. The fine-grained isotropic graphites IG-110 and IG-430, the candidate grades for the VHTR in-core components, were used in this study. The following results were obtained.

- The micro-indentation behavior was changed by applying the compressive strain on the graphite. It suggested that the residual stress in the components could be measured directly by the micro-indentation method. The optimization of the measuring condition to reduce the scattering of experimental data is the important issue and it will be studied in the next step.
- The change of ultrasonic wave velocity with 1 MHz by the uniform oxidation was evaluated by the wave-propagation analysis with wave-pore interaction model. The applicability of the propagation model was expressed.
- The strength evaluation on IG-110 with proposed oxidation model expressed that the trend of oxidation induced degradation can be analyzed. The analysis showed slightly higher values than the experiments, and hence it indicated the importance of the non-uniformity consideration.

## Acknowledgements

This study is the result of contract research in the fiscal year of 2005, 'Research and development for advanced high temperature gas cooled reactor fuels and graphite components', which is entrusted to the Japan Atomic Energy Agency by the Ministry of Education, Culture, Sports, Science and Technology of Japan.

## References

- [1] W. Höffelner, G. Hayner, P. Billot, in: Proceedings of ICAP'05, Seoul, Korea, 2005, Paper 5206.
- [2] K. Sawa, S. Ueta, T. Shibata, et al., Research and development plan for advanced high temperature gas cooled reactor fuels and graphite components (contract research), JAERI-Tech 2005-024, 2005 (in Japanese).
- [3] T. Shibata, S. Hanawa, J. Sumita, et al., in: Proceedings of GLOBAL2005, Tsukuba, Japan, 2005, Paper 360.
- [4] J. Sumita, S. Hanawa, T. Shibata, et al., in: Proceedings of ICONE14, Miami, USA, 2006, ICONE-89384.
- [5] K. Kunitomi, S. Katanishi, S. Takada, et al., Trans. At. Energy Soc. Jpn. 1 (2002) 352.

- [6] S. Saito, et al., Design of High Temperature Engineering Test Reactor (HTTR), JAERI 1332, 1994.
- [7] M. Ishihara, T. Oku, Trans. Jpn. Soc. Mech. Eng. A 62 (1996) 2305 (in Japanese).
- [8] T. Shibata, M. Ishihara, Trans. SMiRT-16, Washington DC, USA, 2001, p. 1114.
- [9] S. Sato, K. Hirakawa, A. Kurumada, et al., Nucl. Eng. Design 118 (1990) 227.
- [10] J. Takatsubo, S. Yamamoto, Trans. Jpn. Soc. Mech. Eng. A 60 (1994) 2126 (in Japanese).
- [11] T. Shibata, M. Ishihara, Nucl. Eng. Design. 203 (2001) 133.
- [12] M. Ishihara, T. Iyoku, J. Toyota, et al., An explication of design data of the graphite structural design code for core components of high temperature engineering test reactor, JAERI-M 91-153, 1991 (in Japanese).